CHAPTER 3

METHOD OF STUDY

3.1 Input Data

In this study, maps relevant to landslide susceptibility analysis were constructed using GIS software Arc Map 9.1 in UTM projection system. To facilitate the data processing and in particular map overlay operations, all data, stored as ARC/INFO files, were first converted from vector to raster structure and then transferred to a raster-based GIS (ArcMap, version 9.1) for subsequent analysis. The data layers used in this study are geologic map, landuse map, streams proximity map and slope map

While rainfall is one of the important triggering factor, the same is not included in the present study. The effect of rainfall in the study area is considered uniform throughout. However, its importance has been reiterated by performing slope stability analysis in later part of this study.

3.1.1 Slope

Slope angle is a major factor influencing the development of landslides in an area (Uromeihy and Mahdavifar, 1999). Slope is the angle formed between any part of the surface of the earth and a horizontal datum. Slope angle is frequently used in landslide susceptibility studies since landsliding is directly related to slope angle

(Anbalagan 1992; Pachauri *et al.,* 1998; and Saha *et al.*, 2002). Landslides mostly occur at certain critical slope angles (Dai *et al.*, 2002). The probability of occurrence of landslide increases as the slope angle increases. A slope map represents areas of equal inclination angle.

The slope map of the area is derived from the Digital Elevation Model (DEM) of the study area with the output cell size of 30 m x 30 m which is constructed using topographic map scale 1:50,000 (Edition -1-RTSD, Series – L7018 and Sheet – 4746 I). A raster layer of continuous angle values was thus generated. The resultant slope map is reclassified into three slope categories viz. less than 15^{o}, $15^{o} - 30^{o}$ and more than 30^{o} (Figure 3.1).

3.1.2 Landuse

The study area has a large area covered by different types of forest. The high coverage of forest is mainly because the study area includes 261 km^2 Doi Suthep-Pui national park which was established on 14 April 1981. Agriculture, in general, is practiced on low lands, although moderately steep and steep slopes are not spared in places. The crops grown in the study area mainly consist of different types of vegetables and high land rice cultivation. Besides having many villages and small towns in the study area the built up area also includes important places like Doi Suthep temple located at 1050 m on the eastside of Doi Suthep, established over 600 years ago and Phuping Palace established in 1961, also located on eastside of Doi Suthep. The study area is also characterized by many streams and reservoir as well. In this study the study area has been classified into four different land use/land cover classes (Figure 3.2).

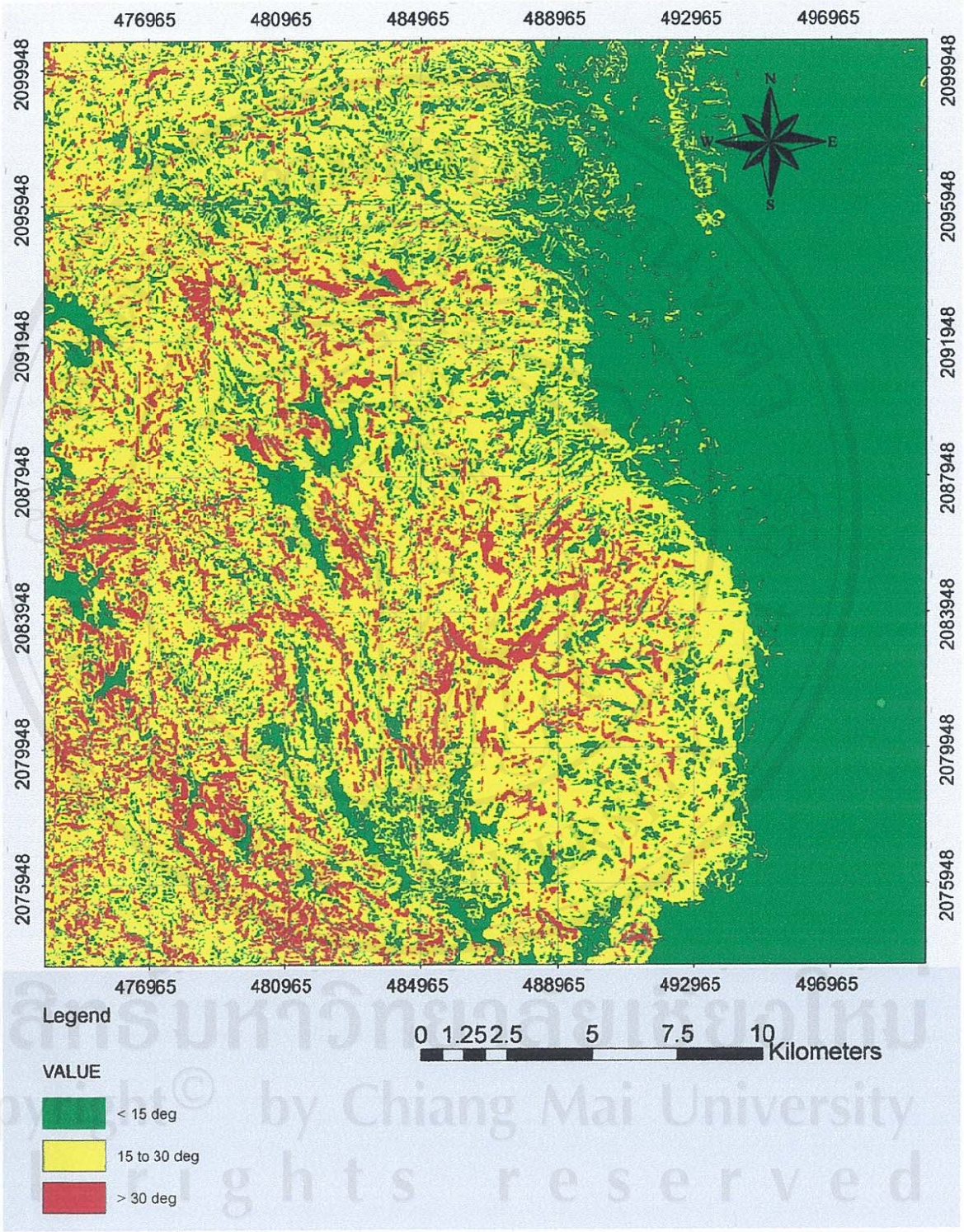

Figure 3.1 Slope map of the study area.

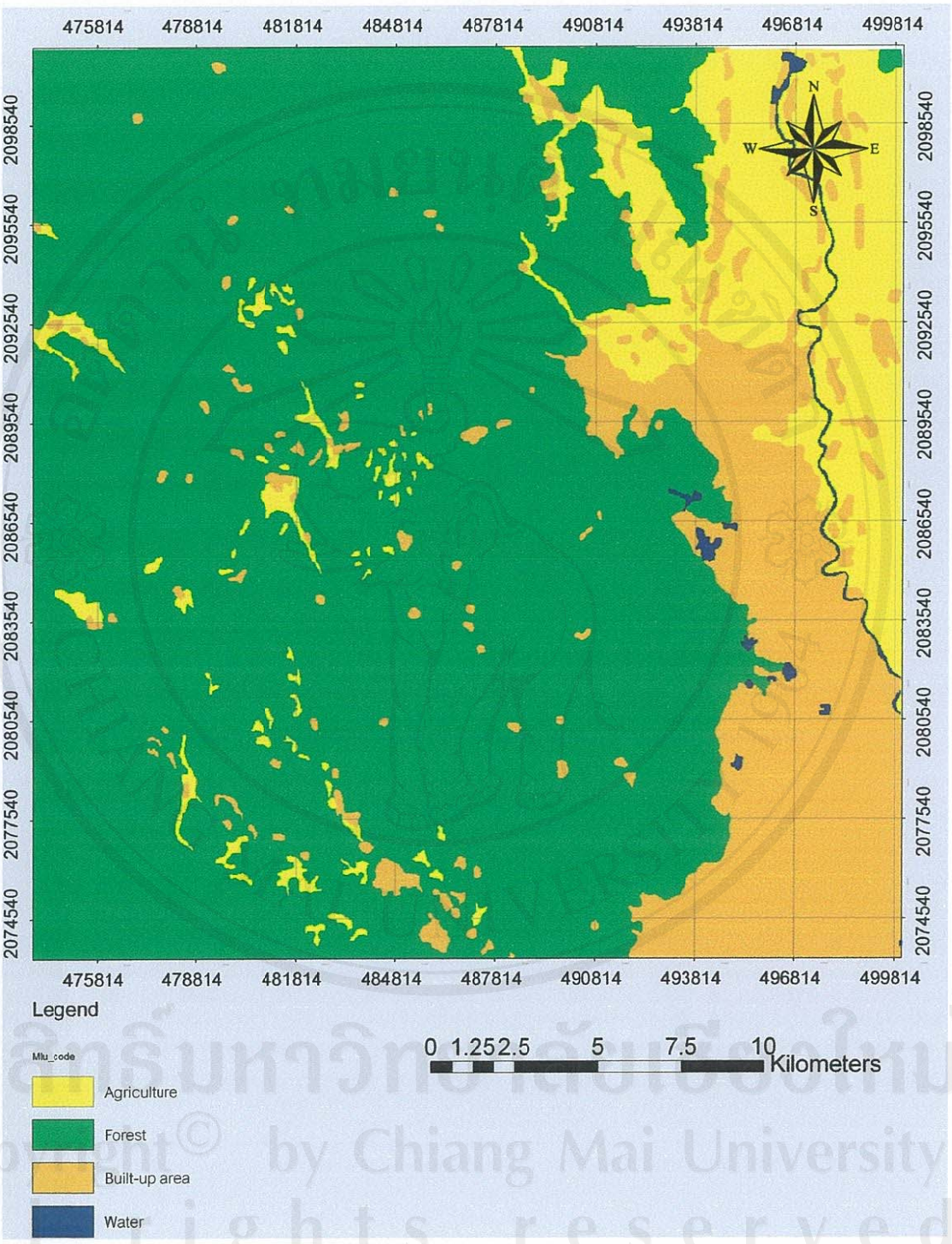

Figure 3.2 Landuse map of the study area.

3.1.3 Stream Proximity

One of the controlling factors for the stability of slopes is the degree of saturation. Streams may adversely affect stability by eroding the toe and/or saturating the slope (Dai *et al.*, 2002). The study area is characterized by mountain ridges and valleys. Almost all valleys have streams of different sizes flowing through.

To create a buffer, first distances to the streams were calculated using the spatial analyst function for raster features. Then the distances were divided into two different buffer ranges. The 50 m on either side of stream forms the first buffer and the distances beyond 50 m forms the second buffer (Saha *et al.*, 2002). The stream proximity map of the study area is given in Figure 3.3.

3.1.4 Geology

Geology plays an important role in landslide susceptibility studies because different geological units have different susceptibilities to active geomorphological processes like landslides (Anbalagan 1992, Pachauri *et al.*, 1998, Dai *et al.*, 2002).

In this study, the Geologic Map of Northern Thailand (Scale 1:250000) Sheet (Chiang Mai) 5 was used. The rock types of the study area were classified in to four groups viz. carbonate rocks, clastic rocks, gneiss and granite, and unconsolidated sediments. The geologic map of the study area is presented in Figure 3.4.

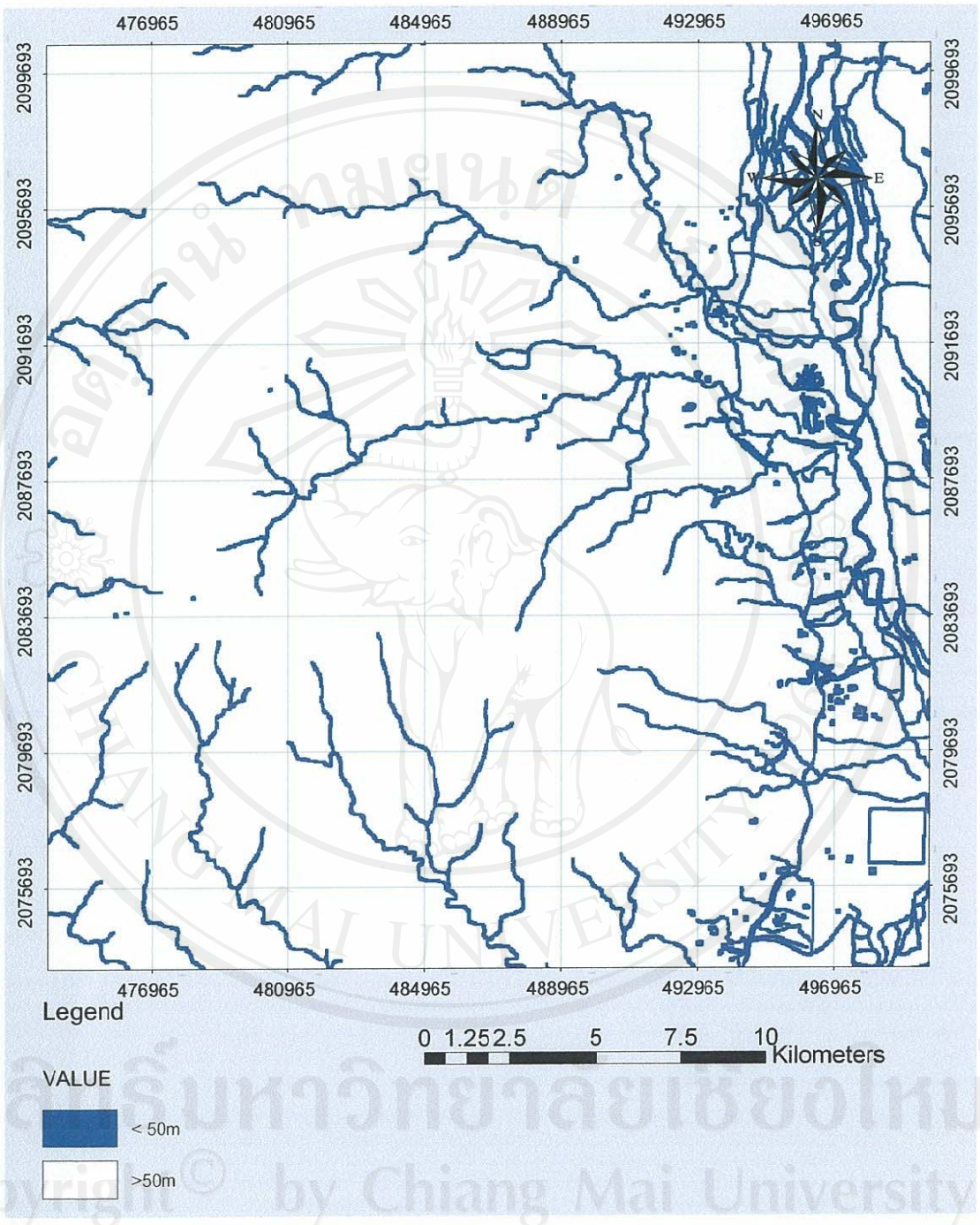

Figure 3.3 Stream proximity map of the study area.

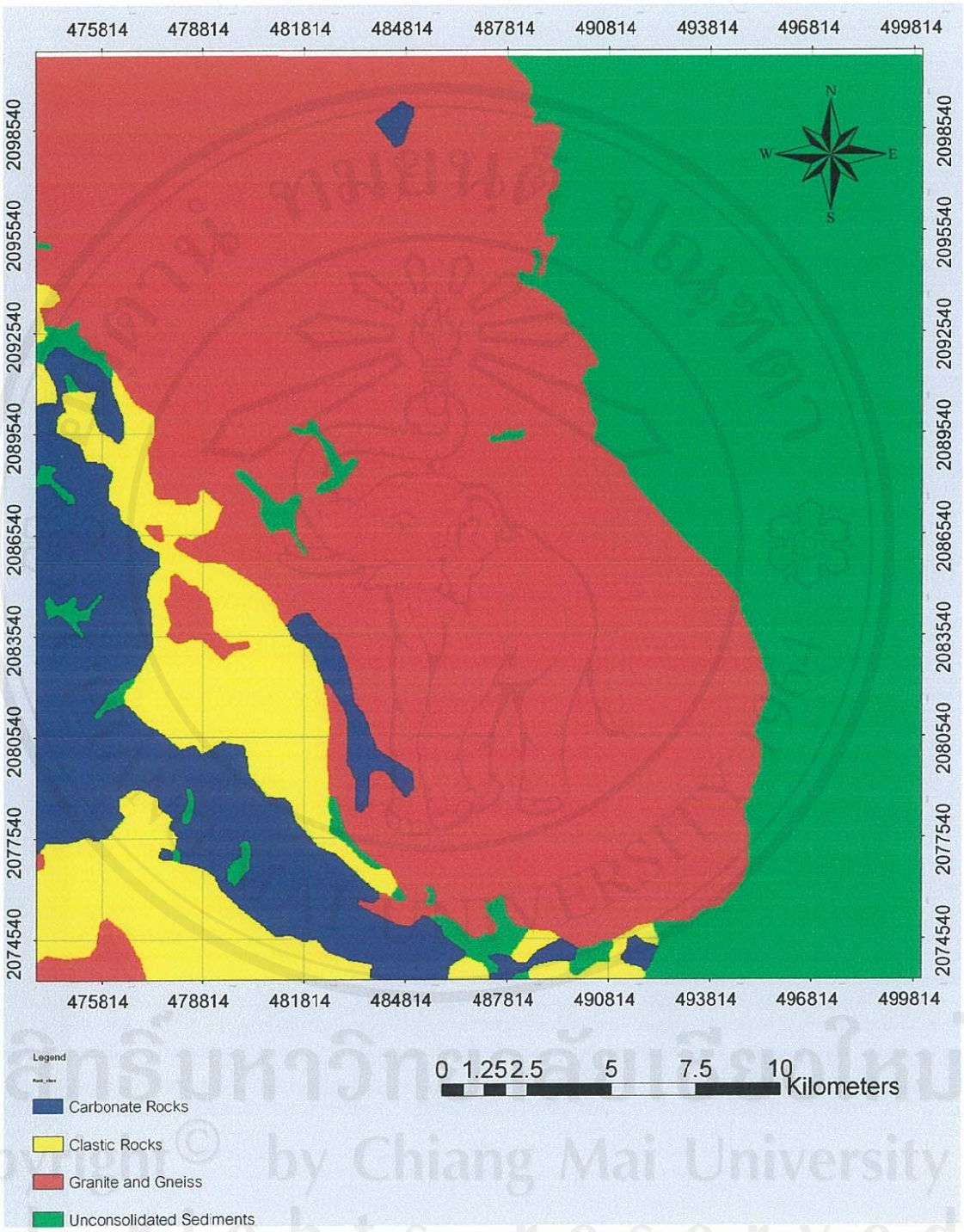

Figure 3.4 Geologic map of the study area.

3.2 Data Integration and Analysis

Landslides are caused by mutual interaction of various factors. The process and exact mechanism are still not well understood (Saha *et al.*, 2002). This makes prediction quite difficult. Therefore, there is a substantial degree of uncertainty involved in any hazard evaluation process. Various methods of data integration for landslide hazard zonation exist. Main types of methods include: landslide inventory method, deterministic method, heuristic method, and statistical method (Varnes, 1984). The data integration method used in this study is heuristic approach. The heuristic approach utilizes data integration techniques, including qualitative parameter combination, in which the analyst assigns relative weighting–rating values to a series of terrain parameters and to each class within each parameter. The parameter layers are then combined within the GIS to produce hazard values. Heuristic methods use selective criteria, which need expert knowledge to be suitably applied. The whole process of data integration and analysis adopted in this study is as presented in Figure 3.5.

3.2.1 Data Layers: Weights and Ratings

Although a variety of procedures exists for establishing parameter weights, the Analytical Hierarchy Process (AHP) makes it possible to evaluate the consistency of the parameters pair-wise comparison. The AHP method, developed by Saaty (1980), is used to define the factors that govern landslide occurrence more transparently and to derive their weights. The weighting system is based on the relative importance of various causative factors derived from field knowledge. In this procedure, a value between 9 ('much more important than'), 1 ('equally important as') and 1/9 ('much

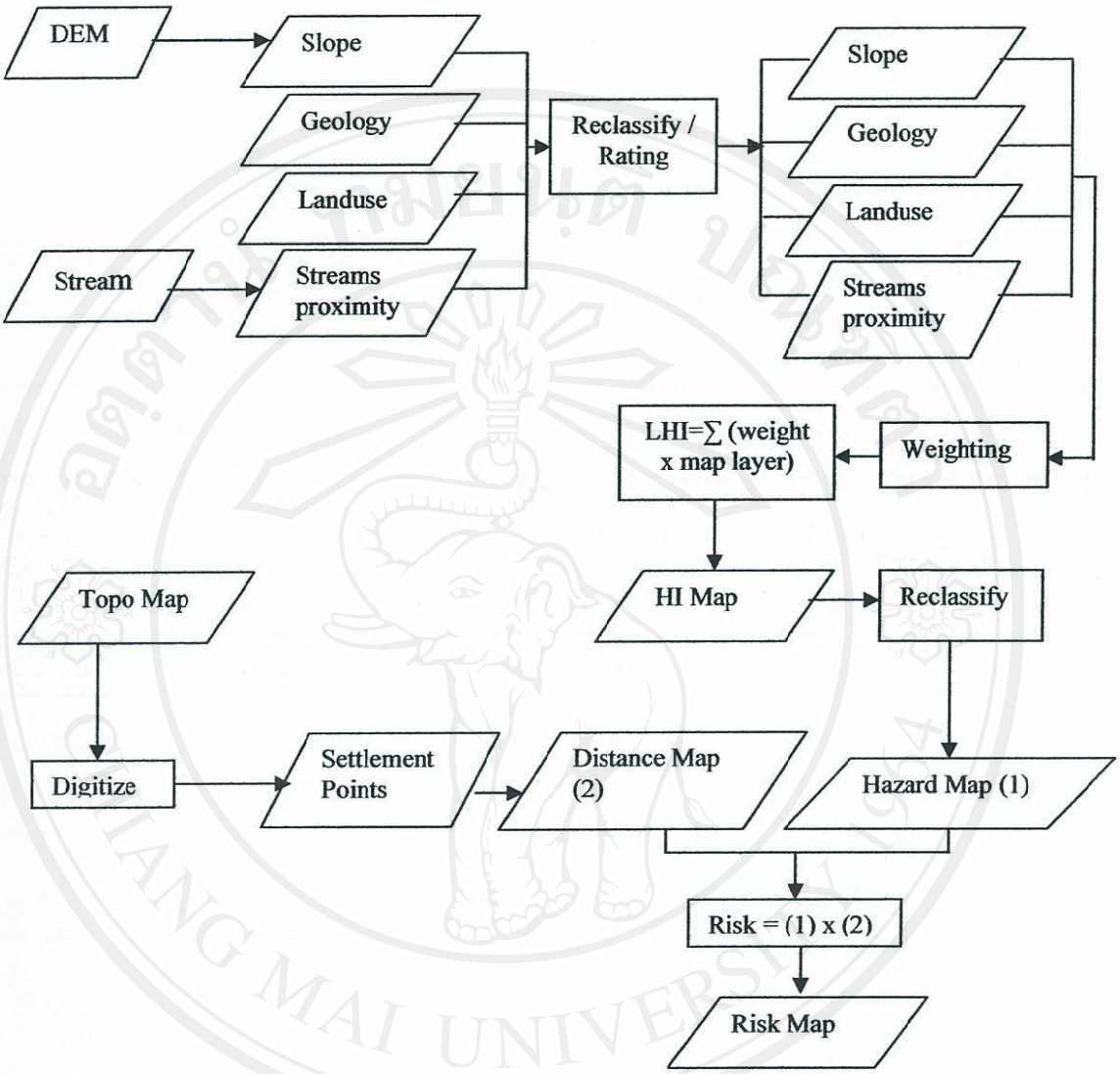

Figure 3.5 GIS analysis for integrating various thematic data layers and deriving landslide zonation and risk map.

less important than'), is assigned to each pair of parameters in a square reciprocal matrix by rating rows relative to columns.

Weights of parameters are derived by taking the principal eigenvector of the parameter matrix. The procedure requires the principal eigenvector of the matrix to be computed to produce a best-fit set of weights. The procedure offers an advantage over

other weighting methods, since it produces a consistency ratio (CR), which reveals the degree of consistency used when developing the weights. The CR indicates the probability that the matrix rating was randomly generated (Barredo *et al.,* 2000). Saaty (1980) suggests that matrices with CR greater than 0.09 for 4x4 matrices should be re-evaluated.

Various input data layers, namely slope map, geologic map, landuse map and stream proximity map were arranged in a hierarchical order of importance, and a weighting number (from 0 to 4) given to each map layer (Saaty, 1980) and the weights are calculated accordingly. Table 3.1 shows the weights obtained based on AHP. The detailed calculation of the weights using AHP is illustrated in Appendix I.

Table 3.1 Parameter weight assignment based on the analytical hierarchy process (Consistency ratio = 0.03)

	Slope	Geology	Landuse	Stream Proximity	Weight
Slope	1.00	2/1	5/2	7/2	0.44
Geology	1/2	1.00	2/1	4/1	0.30
Landuse	2/5	1/2	1.00	2/1	0.17
Stream Proximity	2/7	1/4	1/2	1.00	0.09

Similarly, each class within a layer was given an ordinal rating from 0 to 5. These weights and rating values have been re-adjusted using a trial and error method after repeated desk top study and field investigation. The slope angle is found to be a very important parameter in landslide activity in the study area. Hence the highest weighting is assigned to the slope component. The slopes were divided into three

classes and accordingly corresponding ratings were assigned to the slope classes. The steeper is the slope, the higher is the rating.

Geology also plays a significant role in the area on landslide activity. Among the four parameters, the importance of geology is the second to the slope and was thus weighted the second highest. Field investigation revealed that the granite, gneiss and clastic rocks are vulnerable to landsliding as they form steep slopes coupled with high degree of weathering. Further, several landslides have been observed in these rock types. Hence, these rocks were assigned a higher rating, while carbonate rocks and unconsolidated sediments are assigned comparatively lower weights since carbonate rocks are less prone to landslides, as observed in the field and unconsolidated sediments are usually found on the foothill and plains where the likelihood of landslide occurrence is minimal.

The landuse pattern, which is also an important parameter in the landslide activity, is of the third importance. Various landuse classes considered in this study are water body, agriculture, built-up area and forest. The agricultural area (least vegetated) areas are most prone to landslide activity, and hence the highest rating is assigned to this class. As the vegetation density increases, the stability of slope tends to increase. Hence, relatively lower rating is given to the forest area. As built up being one of the areas prone to landslide, comparatively higher rating is assigned while water body is assigned with the least rating as no landslide is expected to occur inside water.

The distance to streams was considered to take into account the river undercutting which may induce landslides. The proximity to the streams is divided into two classes and high rating is assigned to the buffer zone up to a distance of 50 m

from the stream. Table 3.2 describes the weights and ratings given to each data layer and their classes, respectively.

Table 3.2 Data layers and landslide hazard weighting–rating system adopted

No.	Data layers	Classes	Weighting (%)	Rating
1	Slope angle	A. > 30°	44	5
		B. 15°-30°		2
		C. <15°		1
2	Geology	A. Granite and Gneiss	30	5
		B. Clastic Rocks		5
		C. Unconsolidated Sediments		3
		D. Carbonate Rocks		2
3	Landuse	A. Agricultural land	17	5
		B. Built-up area		4
		C. Forest area		2
		D. Water body		1
4	Stream Proximity	A. < 50 m	9	5
		B. > 50 m		1

3.2.2 Landslide Hazard Index and Hazard Map

Classes of different data layers are assigned the corresponding rating value as attribute information in the GIS and an 'attribute map' is generated for each data layer. These attribute maps are then multiplied by the corresponding weights and then added up to yield the Landslide Hazard Index (LHI). The raster operation capability of GIS has been utilized to compute the LHI. The method used is described by Barredo *et al.* (2000), which integrate various factors in a single hazard index accomplished by a procedure based on the weighted linear sum as follows:

$$LHI = \sum_{i=1}^{n} w_i x_{ij}$$

where:

LHI : landslide hazard index

W_i : weight of parameter i

x_{ij}: rating of class j in parameter i

The above integration of various factors was possible using a raster calculator of Arc GIS. The landslide hazard index values generated are as shown in Table 3.3. The LHI value is found to vary from 147 to 394. The landslide hazard index map generated using the above formula is presented in Figure 3.6. The hazard index values are then reclassified to yield three classes of landslide hazard viz. low, medium and high hazard.

Table 3.3 Landslide hazard index values and hazard classification

Landslide Index	Landslide Hazard Classification
147 - 250	Low Hazard
250 - 310	Medium Hazard
310 - 394	High Hazard

3.2.3 Risk Map

In an ideal situation, the risk map of the area should be generated considering the nature of damages likely to be caused to properties and human lives if the failure occurs (Anbalagan, 1992). However, in this study the risk map is developed considering the location of the villages and important and frequently visited places such as Doi Suthep Temple and Phuping Palace. This consideration makes sense as most of the people (villagers and visitors) and public facilities are located in and around such places.

First, the village points and other important places were digitized using onscreen digitizing technique available in Arc GIS. Distance is calculated from each point. Figure 3.7 shows the location of the places and the distance calculation from each place. The concept used in generating the risk map is that risk is a function of hazard and damage potential (Anbalagan, 1992). The distance map thus produced is reclassified and a buffer of 1 km is created and assigned weights for different classes of distance (Chalermpong, 2002). The smaller the distance from the place the higher is the rating assigned. The resultant map is then multiplied with the hazard map in the raster calculator function and the map thus generated is again reclassified to obtain the risk map.

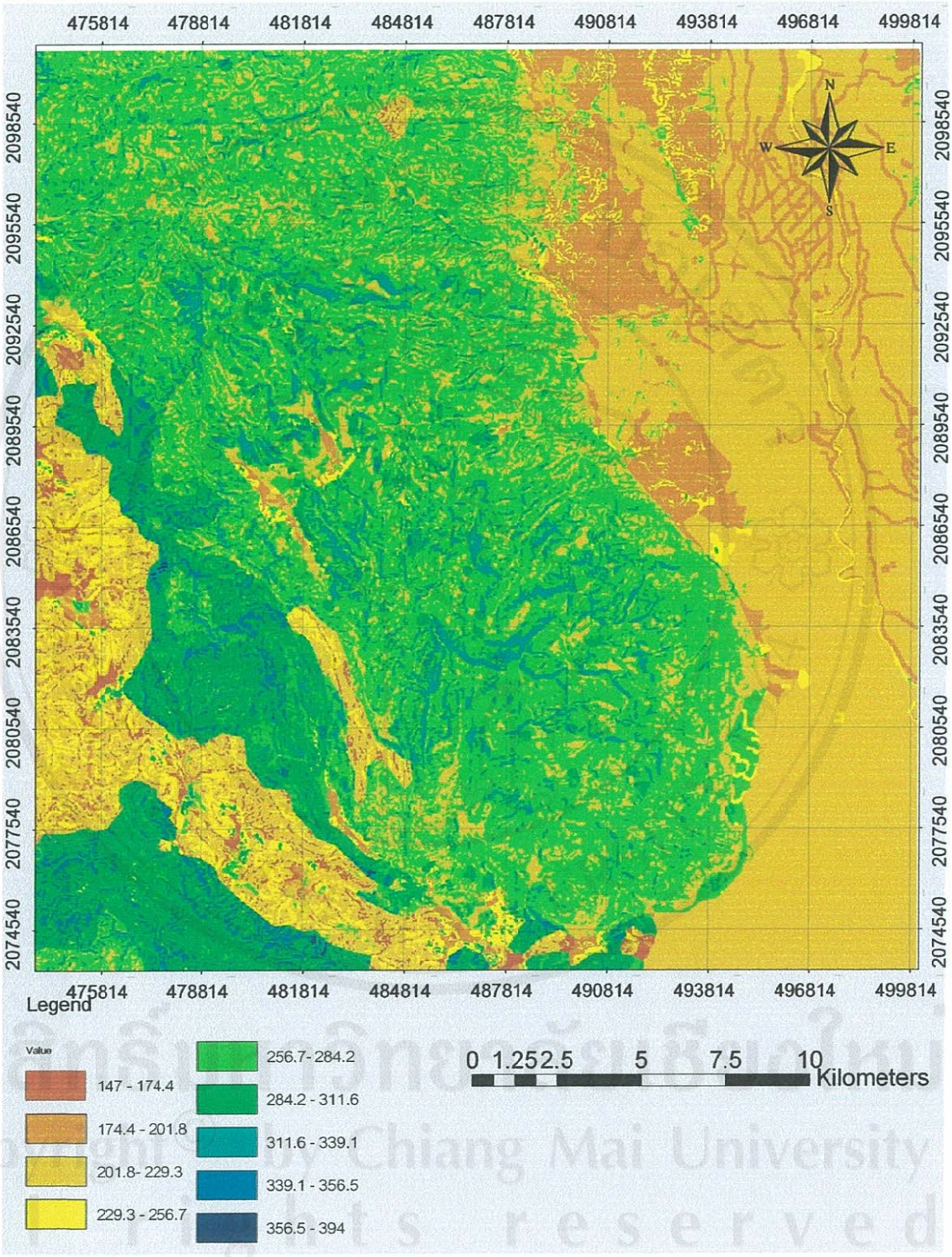

Figure 3.6 Hazard Index map

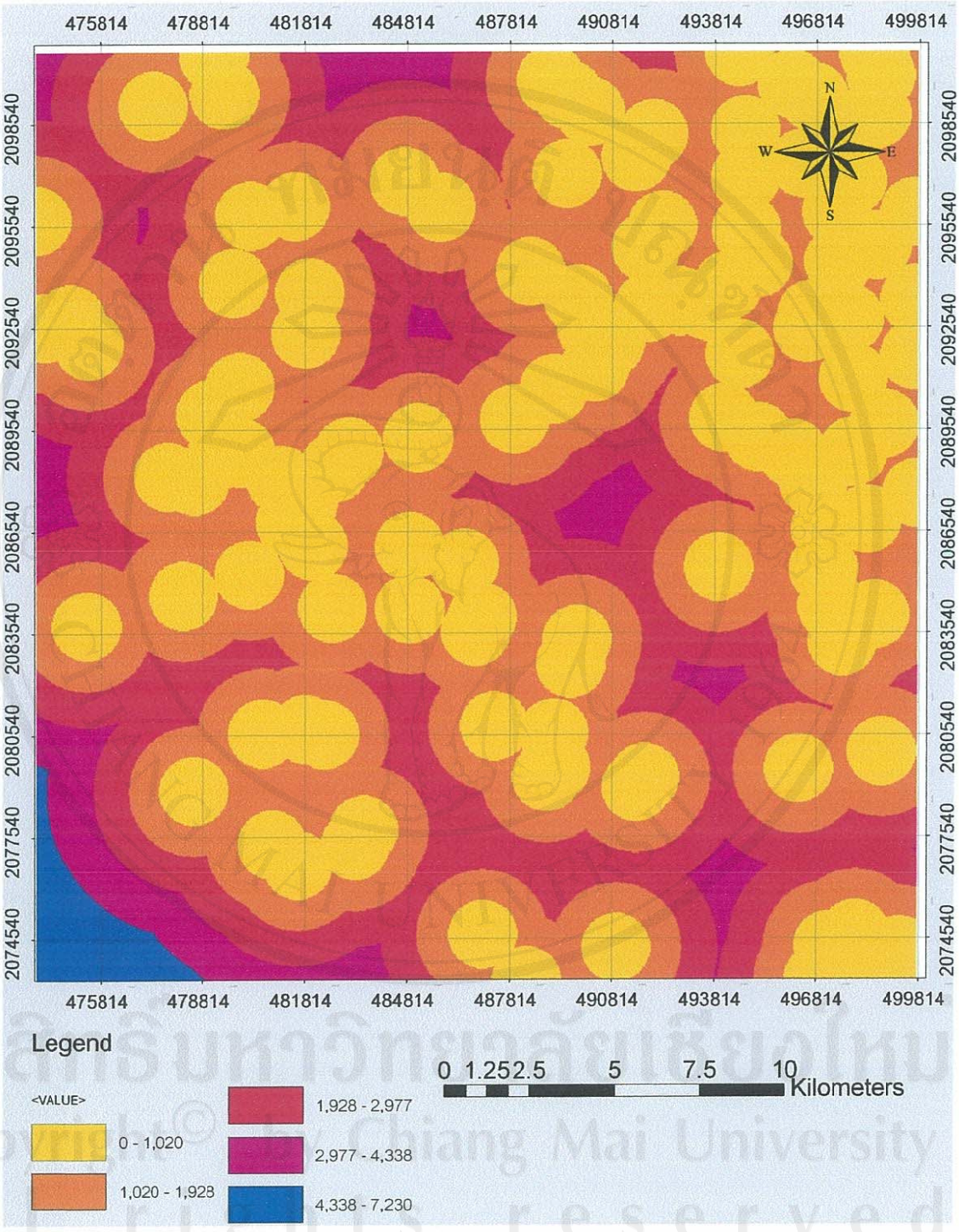

Figure 3.7 Distance to the settlement points

3.3 Field Investigations

Once the hazard map was generated, the field investigation was carried out to check whether or not the hazard map generated fits with the field reality. The field checks include the verification of the location of the existing landslides and collection of geotechnical and hydrological data for slope stability analysis, one each in weathered gneiss and weathered shale. Mapping and detailed study are restricted to along roads and highways because firstly, these are the areas likely to have maximum landslide due to cutting of the slopes to built roads and, secondly, limited time in hand to hike the rest of the area. A special attention was paid to the places with high hazard.

3.3.1 Landslide Mapping

Landslides encountered during the field investigation are geo-referenced using Global Positioning System (GPS) and mapped in the hazard map. Slope (both natural and modified due to road cut) and landslide dimensions are measured in the field. Types of landuse were also field checked. Detailed descriptions of the prevailing conditions of existing landslides area is as shown in Table 3.4. The figure 3.8 shows the geo-referenced landslides mapped on the hazard map. Figure 3.9 through figure 3.17 shows the pictures of each landslide.

Table 3.4 Description of existing landslides

Sl No	GPS Coordinate	Approx. Dimension (m)			Slope (deg)		Landuse type	Rock type	Remarks
		Height	Width	Depth	General	Modified			
1	0485361 2089342	20	15	1 to 2	45	75	Sparsely vegetated	Gneiss	
2	0483547 2089405	30	80	< 2	60	80	Bamboo forest	Gneiss	3 separate slides
3	0481748 2090947	20	30	2 to 3	50	60	Bamboo forest	Gneiss	
4	0481575 2088311	45	15	1 to 2	60	-	Bamboo forest	Gneiss	Natural landslide
5	0477401 2086061	20	60	1 to 2	70	90	Bamboo mixed	Lime-stone	Rock fall
6	0477077 2082343	38	60	5 to 6	35	40	Bamboo mixed	Shale	
7	0477037 2084682	15	10	< 2	40	50	Bamboo mixed	Gneiss	
8	0491800 2078604	15	8	1 to 2	33	50	Forest	Gneiss	
9	0485295 2086369	40	30	2-3	45	-	Bushy	Gneiss	Old landslide

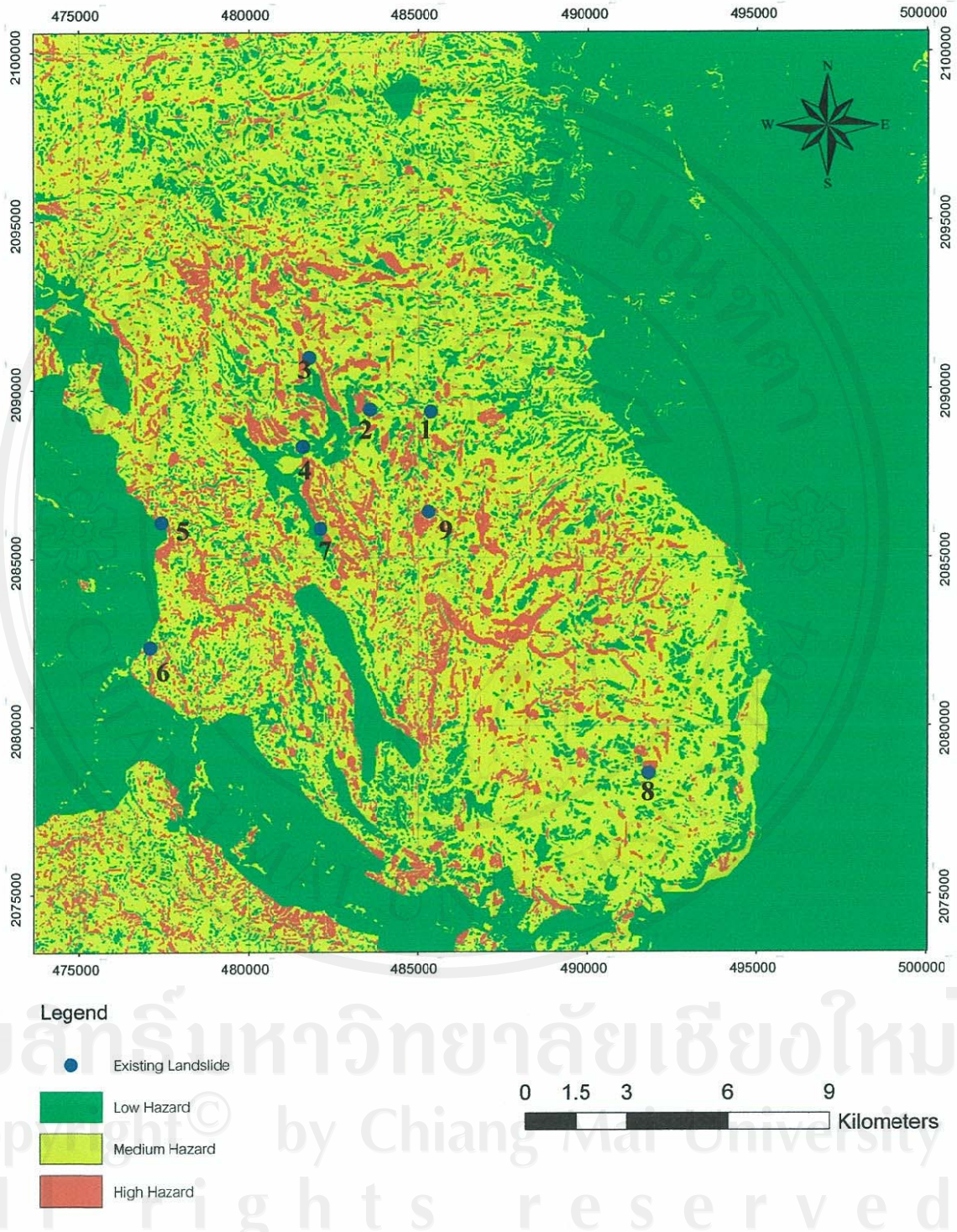

Figure 3.8 Existing landslide mapping

Figure 3.9 Picture of existing landslide (Landslide 1) in weathered gneiss on highway 1096 (Mae Rim-Samoeng highway)

Figure 3.10 Picture of existing landslide (Landslide 2) in weathered gneiss on highway 1096 (Mae Rim-Samoeng highway) near Ban Pong Yaeng Nok.

Figure 3.11 Picture of existing landslide (Landslide 3) in weathered gneiss on road leading to Ban Sam Lang

Figure 3.12 Picture of existing landslide (Landslide 4), a natural landslide in weathered gneiss near Ban Pong Yaeng Nok below highway 1096.

Figure 3.13 Picture of existing landslide (Landslide 5), a rock fall in limestone on highway 1096 (Mae Rim-Samoeng highway).

Figure 3.14 Picture of existing landslide (Landslide 6) in weathered shale on highway 1096 (Mae Rim-Samoeng highway)

Figure 3.15 Picture of existing landslide (Landslide 7), a natural landslide in weathered gneiss above Ban Dong Nok.

Figure 3.16 Picture of existing landslide (Landslide 8) in weathered gneiss before reaching Doi Suthep Temple.

Figure 3.17 Picture of existing landslide (Landslide 9) in weathered gneiss above Ban Mae Sa. The slide occurred in August 2004.

3.3.2 Slope Stability Analysis

Most of the landslides encountered are fresh which occurred during the last monsoon (2006) and are confined to weathered gneiss and shale. To understand the failure mechanism of landslide, slope stability analysis was carried out in weathered gneiss and weathered shale. The slope stability analysis is divided into two parts. The first part focuses on the back analysis of already failed slopes. This analysis is carried out to estimate the water level at which the slope would have failed using Janbu's generalized method of slice. The second part deals with the stability analysis of natural slope to understand and analyze the relation between hydrological conditions and the development of slope movements. The slope stability simulation and modeling was carried out in the natural slope of weathered gneiss and weathered shale

using combined hydrological and stability model (CHASM) software, Version 4.1 (build 413), which is based on Bishop's simplified method of slice.

The input parameters required for both methods of stability analysis were obtained through field and laboratory tests and from the literatures. One undisturbed soil samples each from weathered gneiss and weathered shale (Landslide No. 2 and No. 6 respectively in Figure 3.8) was collected as shown in Figure 3.18. Geotechnical parameters such as friction angle (φ), cohesion (c), field density (γ) and hydrological parameters such as permeability were determined. Direct shear test of soils under consolidated undrained conditions was carried out to determine soil strength parameters, φ and c. The natural water content was also determined. The wet density of soil samples was obtained through field density test while dry and saturated densities of the soil samples were obtained in the laboratory. The permeability of the two soils was also measured at the sites. Rainfall data obtained from Thai Meteorological Department website was used.

Figure 3.18 Sampling site: A – Gneiss and B – Shale, for slope stability analysis

3.3.2.1 Back-analysis of Failed Slopes

The analysis of failed slopes is aimed at determining the effect of water or the height of phreatic surface above the slip surface during the time of the slope failure. Geotechnical parameters required by the Janbu's method of slices were determined through field and laboratory tests. The dimensions of the failed slopes were measured in the field. The profiles of the failed slopes are shown in Figure 3.19.

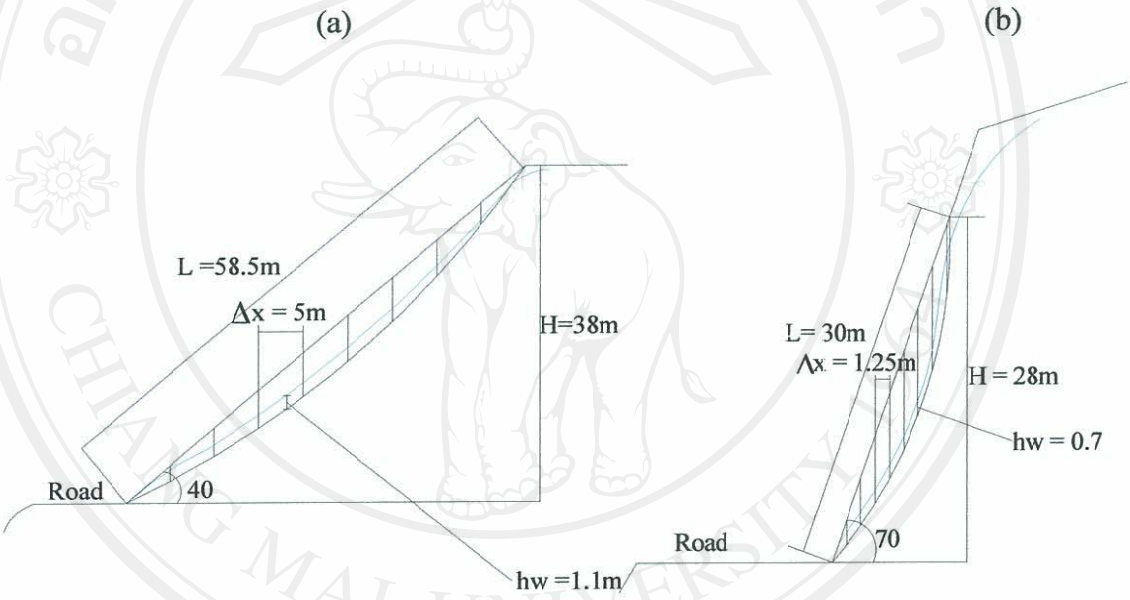

Figure 3.19 Profile of the failed slopes: a) in weathered shale b) in weathered gneiss

Janbu's method for analyzing non-circular failure in slopes is one of the most versatile methods and it is simple enough to permit the solution of problems by hand. When the properties of the soil or waste rock mass vary and the slip surface is not circular as a result to some structural feature such as soil / rock interface, the Janbu's method can be used (Hoek and Bray, 1977). In this method the sliding mass is divided into a number of slices. Unlike other methods, the slices into which the sliding mass is divided need not be of constant width. The factor of safety is given by the formula:

$$FS = f_o \frac{\sum \{c + (p-u)\tan\phi\}\Delta x / n_\alpha}{\sum p.\tan\alpha}$$

Where:

f_o = correction factor

n_α = geometrical functions

c = cohesive strength (kN/m^2)

φ = angle of friction (degree)

p = average weight per unit width of slice (kN)

u = average water pressure on base of slice (kN/m^2)

L = chord length of failure surface (m)

d = depth of failure surface (m)

α = angle of the centre of the base of each slice with respect to the horizontal datum/plane (degree)

Δx = slice width (m)

The inclination α of the center of the base of each slice with respect to the horizontal and the width Δx of the slice are measured. The values of α, Δx, c and φ for each slice are tabulated in Table 3.5 and Table 3.6. The weight of the slice ΔW and the average weight of the slice per unit area of base p are also calculated. Water pressure on the base of each slice is calculated assuming certain value of h_w, which is the height of phreatic surface above base of the slip surface. Thus sum of resisting and driving forces is calculated. Figure 3.20 illustrates a) the section through sliding mass showing slice boundaries and geometrical parameters, b) slice parameters used in the stability analysis and c) calculation of average water pressure u on base of slice.

Table 3.5 Back analysis calculation table for weathered gneiss

											FS (assumed)		1.0	
											FS (calculated)		1.0	
Slice	α	Δx m	hm m	hw m	γsoil kN/m³	c kN/m²	φ deg	p kN/m²	u kN/m²	ΔW	ΔW tan α	X	nα	X/nα
1	83	1.0	2.5	0.7	15.23	15.3	34	38.075	6.86	38.08	309.4	36.3	0.10	379.79
2	75	1.0	7.5	0.7	15.23	15.3	34	114.23	6.86	114.2	425.9	87.7	0.23	375.02
3	74	1.0	7.5	0.7	15.23	15.3	34	114.23	6.86	114.2	398.0	87.7	0.25	346.90
4	72	1.0	7.0	0.7	15.23	15.3	34	106.61	6.86	106.6	327.8	82.6	0.29	283.13
5	70	1.0	5.5	0.7	15.23	15.3	34	83.765	6.86	83.77	230.0	67.2	0.33	202.64
6	68	1.0	4.0	0.7	15.23	15.3	34	60.92	6.86	60.92	150.7	51.8	0.37	139.10
7	60	1.0	2.0	0.7	15.23	15.3	34	30.46	6.86	30.46	52.7	31.2	0.54	57.92
8	55	1.0	0.5	0.5	15.23	15.3	34	7.615	4.90	7.615	10.9	17.1	0.64	26.66
											1905.4			1811.19

Table 3.6 Back analysis calculation table for weathered shale

												FS (assumed)		1.00	
												FS (calculated)		1.00	
Slice	α	Δx m	hm m	hw m	γsoil kN/m³	c kN/m²	φ	p kN/m²	u kN/m²	ΔW	ΔW tanα	X	nα	X/nα
1	55	5.0	1.5	1.0	12.39	10.7	29	18.59	9.81	92.93	132.7	77.8	0.59	131.9
2	50	5.0	4.0	1.1	12.39	10.7	29	49.56	10.79	247.80	295.2	160.9	0.69	234.4
3	45	5.0	5.5	1.1	12.39	10.7	29	68.15	10.79	340.73	340.6	212.4	0.78	273.2
4	40	5.0	5.5	1.1	12.39	10.7	29	68.15	10.79	340.73	285.8	212.4	0.86	247
5	39	5.0	5.5	1.1	12.39	10.7	29	68.15	10.79	340.73	275.8	212.4	0.88	242.7
6	33	5.0	4.5	1.1	12.39	10.7	29	55.76	10.79	278.78	181.0	178.1	0.96	186.1
7	30	5.0	3.8	1.1	12.39	10.7	29	46.46	10.79	232.31	134.1	152.3	0.99	153.8
8	29	5.0	2.3	1.1	12.39	10.7	29	27.88	10.79	139.39	77.2	100.8	1.00	100.8
9	20	5.0	0.8	0.5	12.39	10.7	29	9.29	4.91	46.46	16.9	65.7	1.06	61.86
											1739.4			1632

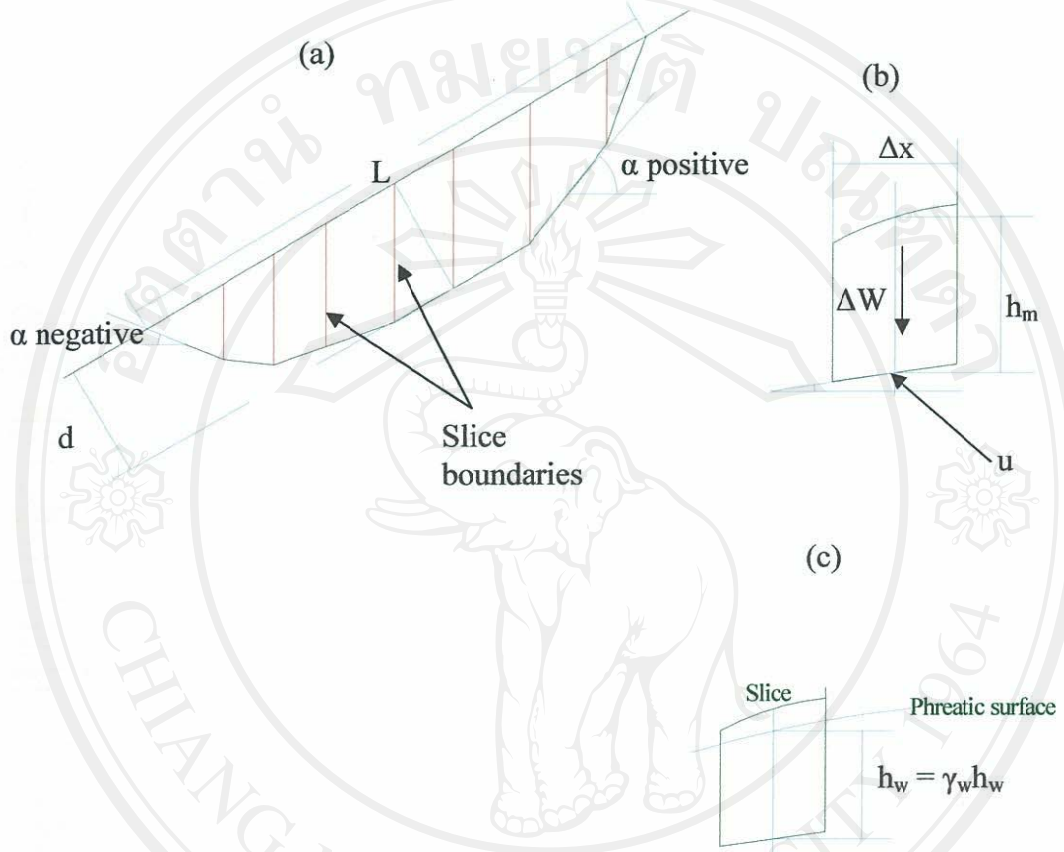

Figure 3.20 Definition of geometrical parameters and method of calculation for Janbu's non-circular failure analysis

After inputting all the parameters in the table, the iteration were performed with different values for h_w each time adjusting the factor of safety closer and closer to 1. The h_w value at the factor of safety equal to 1 is the h_w during the time of the slope failure.

3.3.2.2 Stability Analysis of Natural Slope

Stability analysis of natural slope is carried out using CHASM software. The CHASM is an integrated slope hydrology/slope stability software package that aids the assessment of slope stability conditions. It is designed to help estimate the effect on slope stability of selected storm events, surface covers, slope plan curvatures and other important slope and material properties (Wilkinson *et al.*, 2002).

The dynamics of slope hydrology are computed using a finite difference formulation that accommodates unsaturated and saturated soil conditions. The stability analysis is undertaken using a grid search procedure which is implemented continuously during the simulation period (Wilkinson *et al.*, 2002). The method employed within CHASM 4 is the simplified Bishop's circular stability analysis method with an automated search for the critical slip surface. Figure 3.21 illustrates the definition of geometrical parameters and method of calculation for simplified Bishop's method of slices. The factor of safety is given by:

$$FS = \frac{\sum_{i=0}^{n}\left[c\Delta x_i + (W_i - u_i\Delta x_i)\tan\phi\right]\left[1/M_i(\alpha)\right]}{\sum_{i=0}^{n} W_i \sin\alpha_i}$$

Where $M_i(\alpha) = \cos\alpha_i(1 + \frac{\tan\alpha_i \tan\phi}{FS})$

n = number of slices

FS = factor of safety

c = soil cohesion (kN/m^2)

L = slice length (m)

α = slice angle (degrees)

u = pore water pressure (kN/m^2)

Φ = effective angle of internal friction (degree)

W = total weight of the soil (kN)

Δx = slice width (m) and

θ = slope angle (degree)

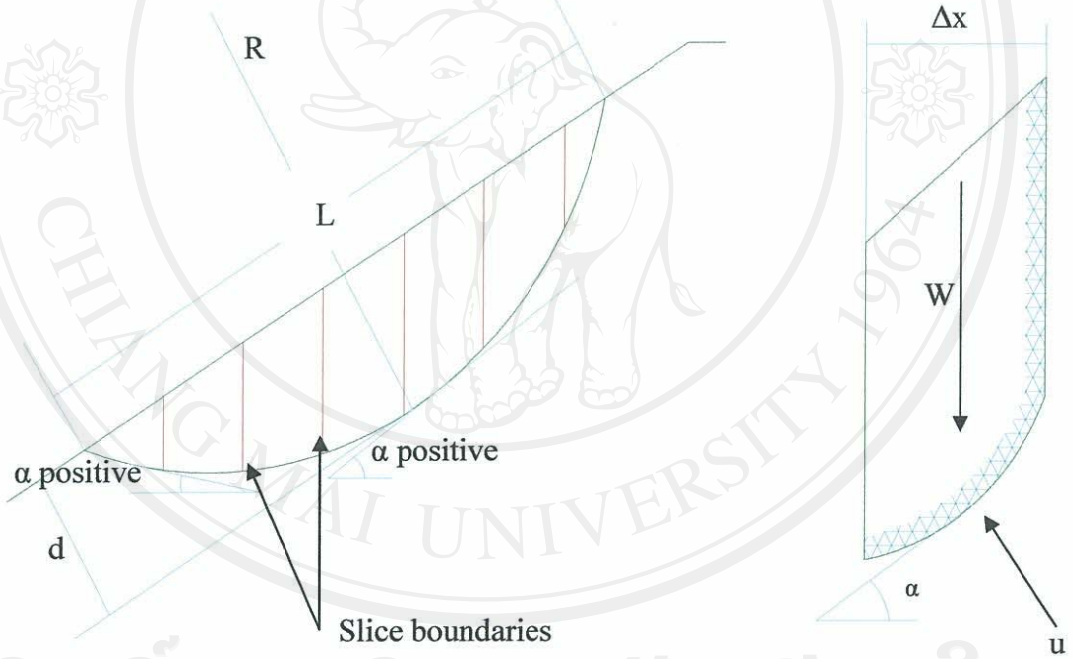

Figure 3.21 Definition of geometrical parameters and method of calculation for Bishop's simplified method of slices

Two natural slopes (Figure 3.22), one near Ban Pong Yaeng Nai and the other near Ban Tong Hua Hin were selected for modeling using CHASM software.

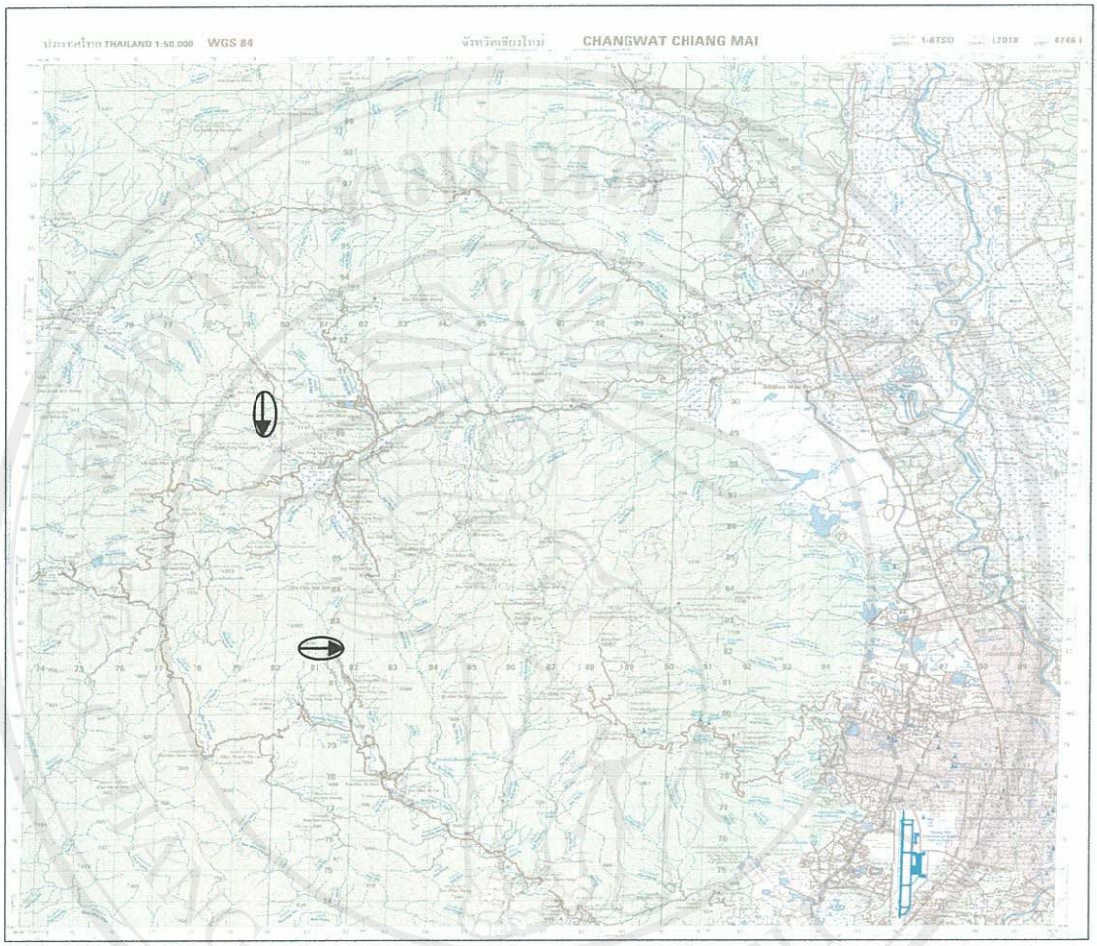

Figure 3.22 Topographic map showing the location and direction of slope under investigation.

The steps outlined in the CHASM 4 HELP has been followed. First the geometry of the slope under investigation, as observed in the field and read from the topographic map was drawn using an automated mesh generator window, which allows drawing a slope profile on the screen, through a simple point and clicking operation (Figure 3.23). From the same window definition of soil layer, water table and choice of slip-circle search grid location (Figure 3.24) for the Bishop's circular stability analysis was achieved.

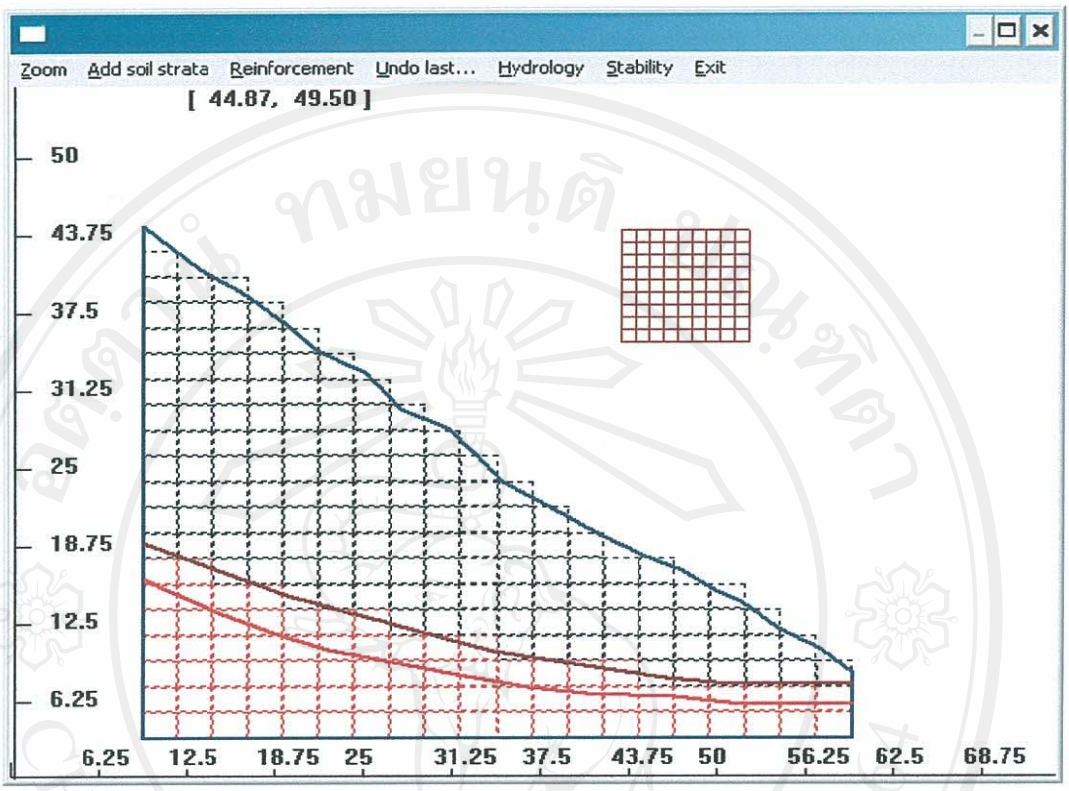

Figure 3.23 On-screen slope geometry and finite difference mesh generation

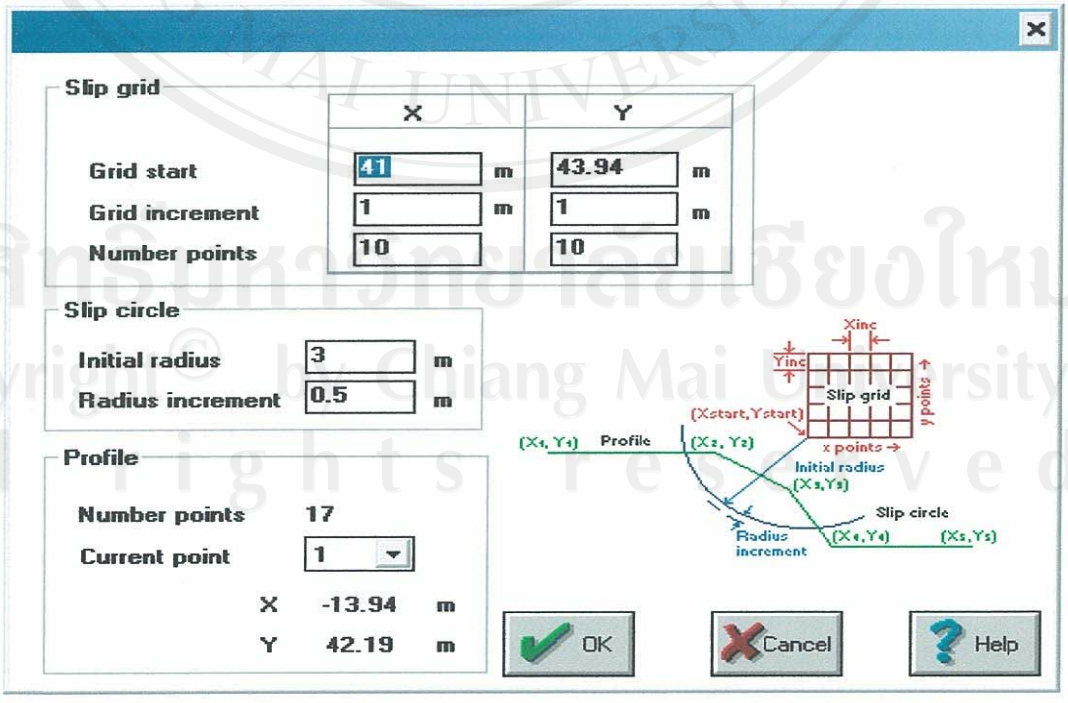

Figure 3.24 Bishop's circular slip search

The second step involved initialization and parameterization of each major component of the model including hydrology, soil and vegetation. In addition to this, other temporal and numerical information such as simulation length and iteration periods were also required. A full list of the model parameters is given in Table 3.7. Initialization and parameterization of the soil, storm and vegetation parameters were done through respective windows. The access to these parameters can also be gained through hydrology summary dialog box (Figure 3.25) which is also used to edit the slope cross- section (including three dimensional slope representations), water table height and the mesh dimension.

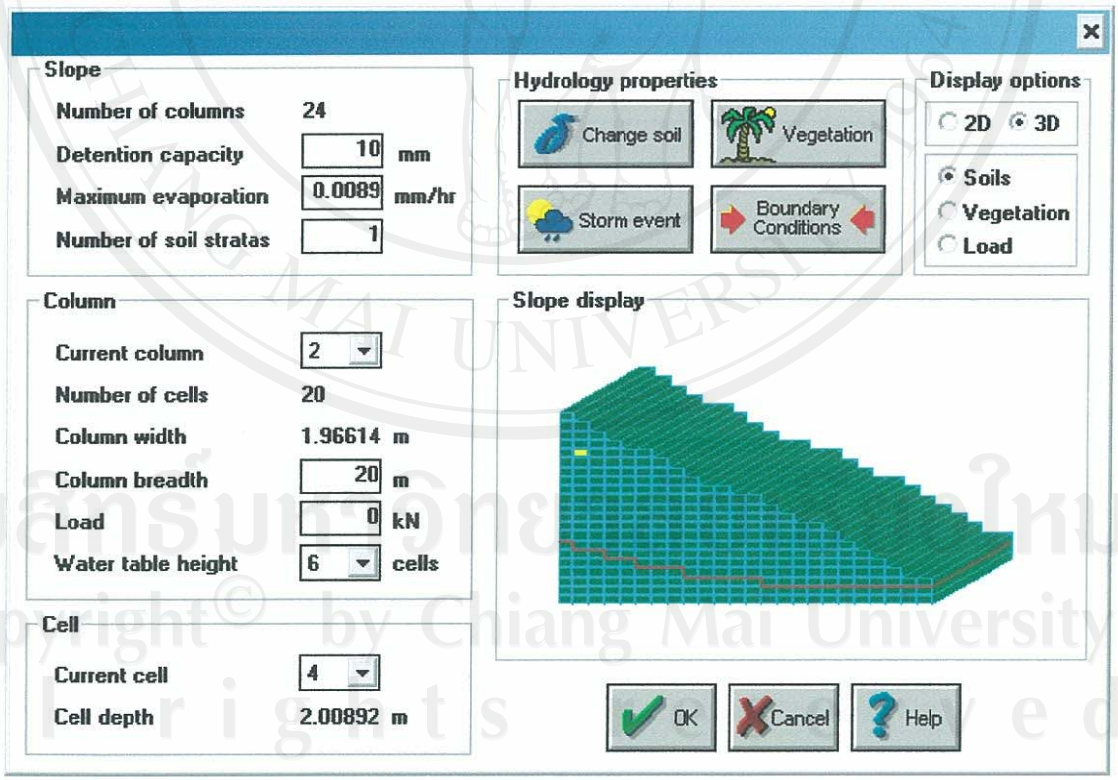

Figure 3.25 Hydrology dialog box (with 3D convergence).

Table 3.7 Input parameters used in back analysis of failed slopes and in natural slopes

Parameter Group	Input Parameter	Unit	Weathered Gneiss	Weathered Shale
Feature geometry	Slope angle	deg	38	31
	Slope length	m	60	60
	Slope height	m	37	32
Soil Properties*	Saturated density (γ_s)	kN/m^3	17.72	15.81
	Wet density (γ_w)	kN/m^3	15.23	12.39
	Dry density (γ_d)	kN/m^3	13.17	9.83
	Cohesion (C)	kN/m^2	15.32	10.69
	Friction angle (φ)	deg	34	29
	Specific gravity (G)	gm/cm^3	2.504	2.575
Hydrology	Permeability (k)	m/sec	$2.16x10^{-6}$	$3.57x10^{-6}$
	Degree of saturation (S)	%	45.88	47.25
	Depth of water table (d)	m	10-20	5-15
	Water content (w)	%	15.84	28.79
	Max. evaporation	mm	0.0005	0.0005
	Rainfall intensity	mm/hr	5	5
	Detention capacity	mm	10	10
	Initial suction in top cell	m	-2	-2
	Simulation period (continuous)	hr	48	48
Numerical	Mesh resolution(width, depth)	m	2,2	2,2
	Iteration period	sec	60	60

* the same properties is used for back analysis of failed slope

On running the program from the main dialog box the option of resetting the initial moisture condition is offered. After making necessary reset the simulation was carried out. During the simulation period, a result window displays the factor of safety, the X-Y coordinates of the slip grid, the slip circle radius and mass of soil above the critical slip surface. These are displayed in real-time (i.e. as the calculations are made), so that the progress of the simulation can be monitored. Once the simulation has finished, the temporal changes in the factor of safety and the position of the critical failure surface were examined (Figure 3.26). Additionally, the spatial distribution of the soil moisture within the slope was examined at the time of the minimum factor of safety by point and click on the finite difference mesh (Figure 3.27)

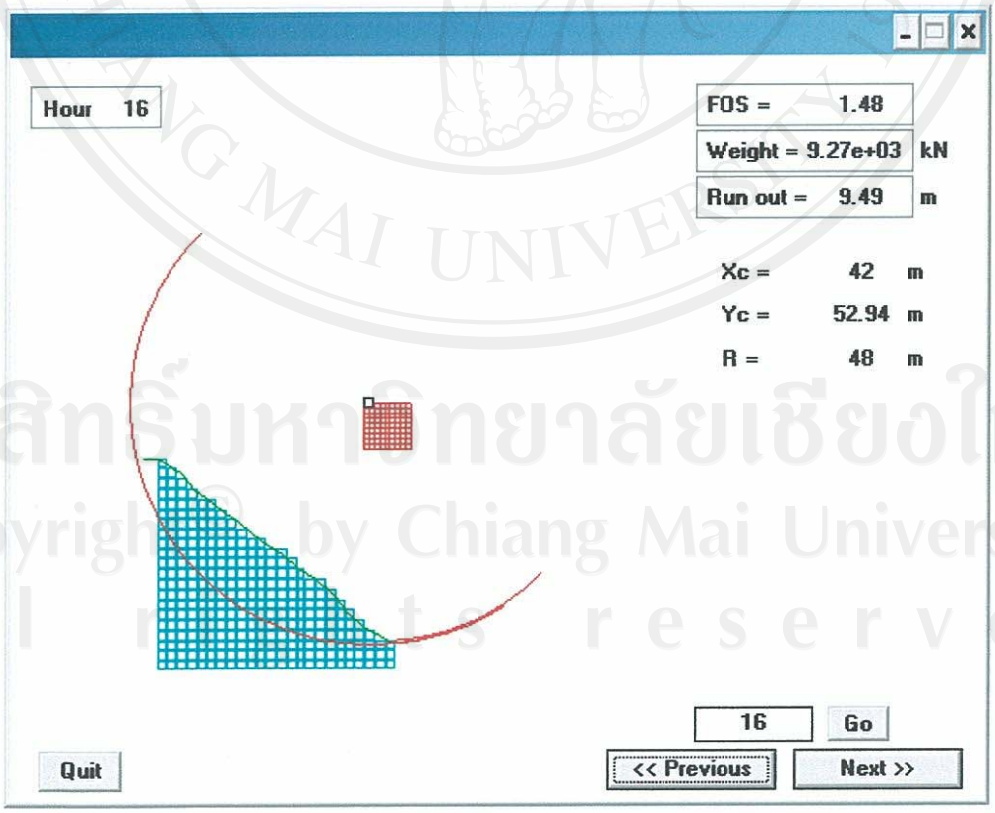

Figure 3.26 CHASM visualization of critical slip surface

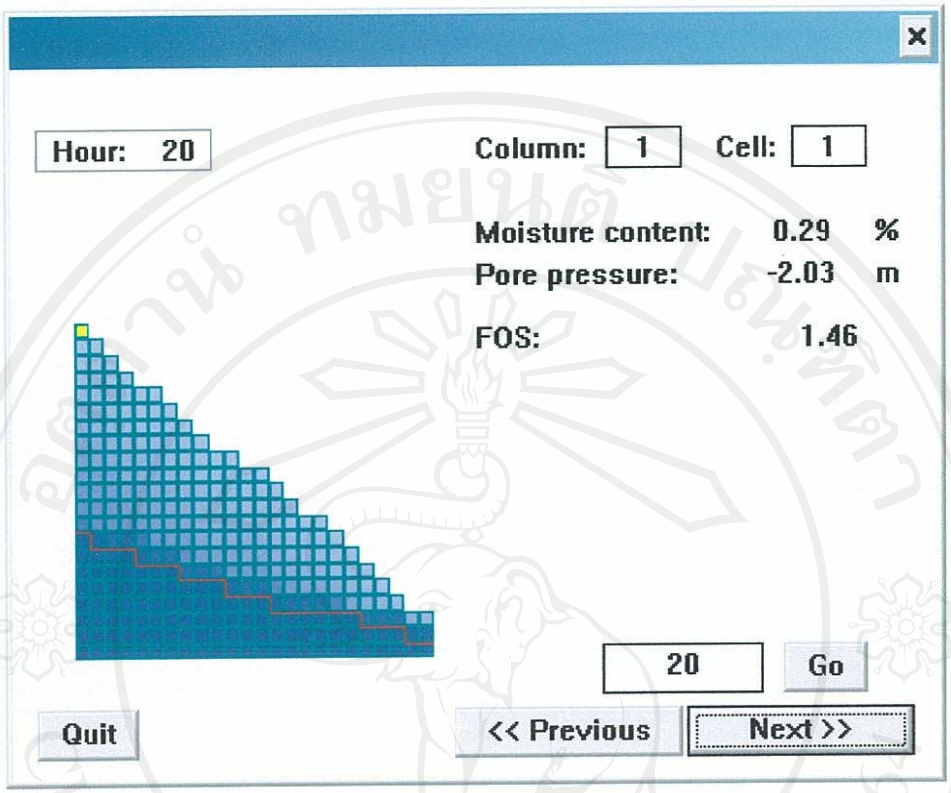

Figure 3.27 CHASM visualization of soil moisture distribution